Effects of heat and drought stress on post illumination bursts of volatile organic compounds in isoprene emitting and non-emitting poplar

Werner Jud[1], Elisa Vanzo[2], Ziru Li[3], Andrea Ghirardo[2], Ina Zimmer[2], Thomas D. Sharkey[3], Armin Hansel[1] and Jörg-Peter Schnitzler[2]

[1] Institute of Ion and Applied Physics, University of Innsbruck, Innsbruck, Austria

[2] Research Unit Environmental Simulation (EUS), Institute of Biochemical Plant Pathology (BIOP), Helmholtz Zentrum München GmbH, Neuherberg, Germany

[3] Department of Biochemistry and Molecular Biology, Michigan State University, East Lansing, USA

Corresponding author: Armin Hansel

University of Innsbruck, Institute of Ion and Applied Physics, Technikerstraße 25, 6020 Innsbruck

phone: +43 (0)512 507 52640, fax: +43 (0)512 507 2932, e-mail: armin.hansel@uibk.ac.at

Abstract

Over the last decades, post illumination bursts (PIBs) of isoprene, acetaldehyde and green leaf volatiles (GLVs) following rapid light-to-dark transitions have been reported for a variety of different plant species. However, the mechanisms triggering their release still remain unclear. Here we measured PIBs of isoprene emitting (IE) and isoprene non-emitting (NE) grey poplar plants grown under different climate scenarios (ambient control and three scenarios with elevated CO_2 concentrations: elevated control, periodic heat and temperature stress, chronic heat and temperature stress, followed by recovery periods). PIBs of isoprene were unaffected by elevated CO_2 and heat and drought stress in IE, while they were absent in NE plants. On the other hand, PIBs of acetaldehyde and also GLVs were strongly reduced in stress-affected plants of all genotypes. After recovery from stress, distinct differences in PIB emissions in both genotypes confirmed different precursor pools for acetaldehyde and GLV emissions. Changes in PIBs of GLVs, almost absent in stressed plants and enhanced after recovery, could be mainly attributed to changes in lipoxygenase activity. Our results indicate that acetaldehyde PIBs, which recovered only partly, derive from a new mechanism in which acetaldehyde is produced from methylerythritol phosphate pathway intermediates, driven by deoxyxylulose phosphate synthase activity.

Key-words: climate change scenarios; grey poplar; *Populus* x *canescens*; VOC; isoprene; acetaldehyde; green leaf volatiles; post illumination bursts; LOX;

Introduction

Acetaldehyde and compounds commonly referred to as green leaf volatiles (GLVs, different C_6 compounds originating from the lipoxygenase (LOX) pathway, like E-2-hexenal, Z-3-hexenal, Z-3-hexenol, etc.), are among the most prominent oxygenated volatile organic compounds (oVOC) in the earth's atmosphere (Guenther et al. 2012). Owing to indirect and direct sources from vegetation and microbial activity, they are frequently detected in different vegetative environments (see e.g. Kesselmeier & Staudt 1999, and references therein).

GLVs are often released in considerable amounts by plants under abiotic stress and herbivory or pathogen infection (Loreto & Schnitzler 2010, Holopainen & Gershenzon 2010, Scala et al. 2013). Their formation process in plant chloroplasts seems to be well understood nowadays: lipases are responsible for the release of linoleic acid (C18:2) and α-linolenic acid (C18:3) from galactolipids of the thylakoid membranes. In a second step, lipoxygenase (9-LOX and 13-LOX (linoleate:oxygen 9- or 13-oxidoreductase)) enzymes induce the degradation of these free fatty acids (Hatanaka 1993). Subsequent action of hydroperoxide lyase (HPL), alcohol dehydrogenase (ADH) and isomerization factors are eventually responsible for a distinct temporal succession of the GLVs released (Fall et al. 1999).

It could be shown that the same GLVs are also transiently released by different plant species after suddenly terminating illumination (Holzinger et al. 2000, Graus et al. 2004, Loreto et al. 2006, Brilli et al. 2011, Ghirardo et al., 2011, Jardine et al. 2012), indicating that a similar mechanism might be involved here. It has been argued that these so called "post illumination bursts" (PIBs) might be caused by fast changes in intracellular pH values and consequently membrane stability after fast light-to-dark transitions (Brilli et al. 2011). In the algae *Eremosphaera viridis* a quick light-to-dark transition leads to a short term (1 - 3 min) acidification of the cytosol (Bethmann et al. 1998). This effect could trigger the activation of LOX, which has its activity optimum at pH- values of 6.3 and 4.5 (Hatanaka 1993). Conversely, fast dark-to-light transitions lead to an alkalization (Bethmann et al.

1998), which might explain why fast, repeated light-to-dark transitions don't cause PIBs, as has been shown previously using grey poplar leaves (Graus et al. 2004).

Experiments of Graus et al. (2004) and Jardine et al. (2012) revealed that GLV PIBs are strongly reduced when grey poplar leaves or mesquite (*Prosopis* spec.) branches, respectively, are kept under anoxic conditions. This is consistent with the supposed fatty acid degradation mechanism, since LOX activity requires oxygen.

Along with the GLVs, also acetaldehyde is emitted after leaf-cutting, during drying or leaf collapse under high temperature (Fall et al. 1999, Holzinger et al. 2000, Brilli et al. 2011, Behnke et al. 2013); transient acetaldehyde emissions have been detected after root flooding (Kreuzwieser et al. 2000, 2001) and after light-to-dark transitions (Holzinger et al. 2000, Karl et al. 2002, Brilli et al. 2011, Ghirardo et al. 2011, Jardine et al. 2012). Acetaldehyde emissions after root flooding are explained by an interconversion of ethanol formed in anoxic roots or stems. Root ethanol is transported to the leaves by the transpiration stream and then oxidized to acetaldehyde (by ADH) and eventually by aldehyde dehydrogenase (ALDH) to acetate (Kreuzwieser et al. 1999, 2000).

Though there seems to be an apparent correlation between GLV and acetaldehyde emission after wounding and light-to-dark transitions, the underlying mechanisms are probably different. For acetaldehyde PIBs, some investigations were proposing a "pyruvate overflow mechanism" (Karl et al. 2002, Hayward et al. 2004). Cytosolic pyruvate was thought to increase transiently, thus lowering the cytosolic pH, due to a decreased pyruvate import into the organelles after darkening. When a threshold pyruvate concentration is reached, pyruvate decarboxylase (PDC) starts to convert pyruvate into pH neutral acetaldehyde, preventing acidification of the cytosol (Kimmerer & MacDonald 1987, Harry & Kimmerer 1991). Consistent with this pyruvate overflow theory, the inhibition of mitochondrial respiration and pyruvate transport, thus increasing pyruvate concentrations in the cytoplasm, induced acetaldehyde emissions (Karl et al. 2002).

With the same line of reasoning Jardine et al. (2012) explained the release of post illumination acetaldehyde, ethanol, acetic acid and acetone from mesquite branches in what they termed "pyruvate dehydrogenase (PDH) bypass pathway". In mitochondria of yeast and mammals, PDH catalyses the formation of acetyl coenzyme A (CoA) from pyruvate (see Wei et al. 2009 and references therein). In the PDH bypass mechanism, acetaldehyde is converted into acetate, which can serve as substrate for acetyl CoA synthesis in the chloroplasts. Acetyl CoA is a building block of fatty acids (Boubekeur et al. 2001, Wei et al. 2009) and together with the GLV Z-3-hexenol it can form Z-3-hexenyl acetate in a reaction catalysed by an acyl transferase (D'Auria et al. 2007). Consistently, in $^{13}CO_2$ labelling experiments with cottonwood (Karl et al. 2002), mesquite branches (Jardine et al. 2012) and grey poplar (Ghirardo et al. 2011) it was found that post illumination acetaldehyde partially (60%, 40% and 30%, respectively) originates from recently assimilated carbon. In mesquite branches this was also the case for post illumination acetic acid, acetone, ethanol and the acetate moiety of Z-3-hexenyl acetate (Jardine et al. 2012).

Graus et al. (2004) speculated that acetaldehyde emissions after fast light-to-dark transitions are not directly related to pyruvate, but rather to acetyl CoA. Similar to Jardine et al. (2012) they observed enhanced acetaldehyde PIBs when poplar leaves were kept under anoxic conditions. These enhanced bursts were interpreted as acetaldehyde released from excess acetyl CoA in the case of missing hexenal from the LOX pathway to form hexenyl acetate. In their experiments acetaldehyde PIBs were absent when the light was switched on again before the burst normally appeared. Switching on and off light repeatedly within sub-minutes time spans, thus mimicking so-called light flecks in a natural environment, did not result in any PIBs at all.

Carbon isotope analysis of acetaldehyde emitted from leaves (of poplar, white oak, red maple and sassafras) after mechanical stress led Jardine et al. (2009) to the conclusion, that acetaldehyde is produced by fatty acid peroxidation reactions initiated by the accumulation of reactive oxygen species (ROS). Due to a kinetic isotope effect in the acetyl CoA formation from pyruvate by PDH,

acetyl CoA-derived products like said fatty acids are depleted in ^{13}C (Park & Epstein 1961, DeNiro & Epstein 1977). Jardine et al. (2009) argued that acetaldehyde was as depleted in ^{13}C as these unsaturated lipids, while acetaldehyde derived from ethanolic fermentation, typical under anoxic conditions (e.g. after root flooding, in O_2- free enclosure systems), would be less depleted (Hobbie & Werner 2004). Likewise, acetaldehyde released in leaf heating experiments seems to derive from a bulk biomass precursor, as carbon isotope analysis by Keppler et al. (2004) demonstrated.

Similar to acetaldehyde and the GLV, also isoprene PIBs have been reported in isoprene emitting plant species (Monson et al. 1991, Li et al. 2011, Li & Sharkey 2013). There is now evidence to suggest that the accumulation of methylerythritol phosphate (MEP) pathway intermediates, primarily methylerythritol cyclodiphosphate (MEcDP), is responsible for the post illumination isoprene burst phenomenon (Li & Sharkey 2013). The conversion of MEcDP to dimethylallyl diphosphate (DMADP) and isopentenyl diphosphate (IDP), catalysed by the iron-sulphur protein hydroxymethylbutenyl diphosphate (HMBDP) synthase, is strongly dependent on the electron transport of the photosynthetic light reaction. In darkness, HMBDP synthase switches over time to NADPH as its electron donor (Seemann & Rohmer 2007), thus relieving the intermediate pool and eventually causing the isoprene PIB in naturally isoprene emitting plants.

Aim of the present study was to elucidate the combined effects of heat and drought stress and elevated CO_2 concentration on the different post illumination emissions of volatile organic compounds (VOCs) from isoprene emitting (IE) and isoprene non-emitting (NE) poplar leaves. In NE plants, the knockdown of isoprene synthase (Behnke et al., 2007) affects early metabolites of the plastidic isoprenoid pathway (Ghirardo et al., 2014) and lipid substrates of the LOX enzymes (Velikova et al., 2015). We used the combination of different biochemical and isoprene emission capabilities of IE and NE plants, in conjunction with the different stress-induced responses, to deepen our understanding of the biochemical mechanisms responsible for the post illumination burst of acetaldehyde and GLVs. Moreover, we tested the hypothesis that the amount of VOCs

released in form of PIBs provides another indicator on the plant stress status and related biochemical phenomena in the plant.

Material and Methods

Plant material and climate change scenarios

A detailed description of the plant material and growth conditions of the plants used in this analysis is given in Vanzo et al. (2015); therefore, only a brief summary is given here.

Four different genotypes of *Populus* x *canescens* (Aiton.) Sm. (INRA clone 7171- B4; syn. *Populus tremula* x *Populus alba*) were investigated: two isoprene emitting lines (one wild-type (WT) and one PcISPS:GUS/GFP line in which the PcISPS (*P.* x *canescens* isoprene synthase) promotor was fused to the β-glucuronidase (GUS) and green fluorescence protein (GFP) reporter genes (for details see Cinege et al. 2009)) and two well-characterized non isoprene emitting lines (35S::PcISPS-RNAi lines RA1 and RA2 (see Behnke et al. 2007, Way et al. 2013)).

The plants were grown in four walk-in-size phytotron chambers at the phytotron facility of the Helmholtz Zentrum München. Each chamber contained four sub-chambers, where plants of one genotype (WT, PcISPS:GUS/GFP, RA1 or RA2) were grown (see Supplemental Fig. S1a). In each of the chambers a different environmental scenario was simulated: present and future controls (daily maximum temperature of 27 °C, no stress episodes) and two stress scenarios with periodic and chronic exposure to increased temperatures (T = control temperature +6 °C, daily maximum temperature of 33 °C) and water limitation (see next paragraph). The scenarios are termed as follows:

1. AC: control with ambient $[CO_2]$ = 380 µL L^{-1}.
2. EC: control with elevated $[CO_2]$ = 500 µL L^{-1}.

3. PS: periodic stress containing three cycles (each 6 days) with increased temperature and concomitant, acute drought (hereafter referred as heat and drought spell, HDS). The start of the 1st HDS is termed as day 1 (d1) of the experiment. Between the 1st and 2nd and the 2nd and 3rd HDS a recovery time of two days was implemented, where temperature declined to control level (27 °C) and plants were irrigated to pot capacity.

4. CS: chronic stress with slowly developing drought progressing over 22 days from d0 to d22 (during these days temperature was increased as in PS).

The HDS in the CS and PS scenarios were followed by a final recovery time of 7 days (from d22 to d29) where temperature decreased to control level and pots were irrigated to saturation. These scenarios were considered separately and termed:

5. CSr: recovery from CS scenario.

6. PSr: recovery from PS scenario.

In the CS/CSr and PS/PSr scenarios the ambient CO_2 concentration was the same as in EC ([CO_2] = 500 $\mu L\ L^{-1}$).

In our analysis, the EC scenario is the direct control of the CS/CSr and PS/PSr scenarios. There was no attempt to separate temperature and drought factors in this study.

Plant irrigation and simulation of water scarcity

The controlled water regime was obtained using automated drip irrigation systems placed in each pot half way between the stem and the edge of the pot. Plants were exposed to the short-term (in PS) and long-term drought (in CS) by reducing the amount of irrigation water gradually during each HDS. In the PS scenario, three drought cycles were imposed to mimic natural wet-dry cycles in the field. In the 1st, 2nd and 3rd cycle the amount of water was reduced by 50%, 60% and 70% compared

to AC and EC, respectively. To slow down the progression of drought in the CS scenario, in the first 5 days the irrigation amount was reduced by only 30% compared to fully watered controls in AC and EC. Every 5 days the water amount in CS was reduced by 10% reaching a reduction of 70% compared to the controls.

Leaf-level gas exchange measurements and VOC analysis

Leaf-level gas exchange measurements were made from d19-d22 (during HDS) and d25-d28 (during recovery from HDS). The measurements were performed using two Walz GFS-3000 leaf cuvette systems (8 cm^2 clip-on-type, Heinz Walz GmbH, Effeltrich, Germany) run in parallel. The GFS-3000 systems logged leaf temperatures, pressures, flows, $[CO_2]$, $[H_2O]$ and plant physiological parameters (assimilation rate (A), transpiration rate (E) were calculated automatically). The outlets of the leaf cuvettes were passed by a heated line (T = 40 °C) to a Proton Transfer Reaction Time-of-Flight Mass Spectrometer (PTR-ToF-MS, Graus et al. 2010), see Supplemental Fig. S1b.

The measurements were performed in total on 256 attached leaves (leaf no. 9 counting from the apex) under standard conditions (temperature of 30 °C, photosynthetically active radiation PAR = 1,000 μmol m^{-2}s^{-1}, air humidity of 10,000 ppmv). The cuvette was flushed with synthetic air with growth $[CO_2]$ (AC: 380 μL L^{-1}; else: 500 μL L^{-1}). Each measurement took 40 min, split into three time ranges: (i) 10 min leaf measurement under light conditions, (ii) 20-25 min under dark conditions and (iii) 5-10 min background measurement of the empty cuvette without leaf and light (blank for the PTR-ToF-MS). While sampling from one cuvette, a plant for the subsequent measurement could be installed in the other cuvette and was allowed to acclimatize for 40 min before the measurement began.

The PTR-ToF-MS was operated under standard conditions, 60 °C drift-tube temperature, 540 V drift voltage and 2.3 mbar drift pressure, corresponding to an E/N of 120 Td (E being the electric field

strength and N the gas number density; 1 Td = 10^{-17} V cm^2). The instrument was calibrated once a week by dynamic dilution of VOCs using a standard gas mixture (Apel Riemer Environmental Inc., Broomfield (CO), USA), containing 20 compounds of different functionality distributed over the mass range of 30 - 204 amu. Limits of detection were as low as 35 pptv. Full PTR-ToF-MS mass spectra were recorded up to mass to charge ratio m/z 315 with a 1 s time resolution. Raw data analysis was performed using the routines and methods described elsewhere (see Müller et al. 2013, and references therein).

In PTR-ToF-MS, acetaldehyde can be detected at m/z 45.034, ethanol at m/z 47.050 and isoprene at m/z 69.070. Certain substances like longer-chain aldehydes and alcohols are prone to fragment during the ionization in the drift tube of a PTR-MS (see e.g. Fall et al. 1999) and therefore, the GLVs can be detected at various mass-to-charge ratios, e.g.:

- E-2-hexenal: m/z 99.081, m/z 81.070, m/z 57.034
- Z-3-hexenal: m/z 99.081, m/z 81.070
- Z-3-hexenol: m/z 101.097, m/z 83.086
- Z-3-hexenyl acetate: m/z 143.107, m/z 83.086

PIB signals were background and baseline corrected and quantified by calculating the individual burst area, i.e. the cumulative sum of the ion signal (given in normalized counts per second, ncps) of the burst, normalized to the single-sided leaf area in the leaf cuvette (8 cm^2). Additionally, slopes in the inflection point of the rising edges of PIBs (using a simple linear regression model), the time difference between switching off the light in the cuvette and the burst maxima were calculated. For methanol (m/z 33.034) and isoprene, steady-state standard emission rates normalized to unit leaf area (nmol m^{-2} s^{-1}) were calculated from the last 10 min before switching off the light.

Enzyme extraction and LOX activity analysis

The LOX activity (EC 1.13.11.12) was measured following the protocol described in Koch et al. (1992). Leaf material (leaf no. 9-12 counting from the apex) of IE and NE plants was harvested at noon at the last day of stress treatment and seven days later at the end of the recovery period. Leaves were immediately frozen in liquid N_2 and stored at -80 °C until biochemical analyses. One-hundred mg of leaf material was homogenized with 50 mg Polyclar AT (Sigma Aldrich, Deisenhofen, Germany) on ice in 1 mL PEB (50 mM KP_i pH 7.0; 0.1% (v/v) Triton X-100 and 20 mM DTT). After thoroughly mixing, the homogenates were centrifuged for 15 min at 16,000 g and 0.5 mL of supernatant were loaded on a pre-prepared NAP-5 column equilibrated and eluted with 1 mL of KP_i (50 mM, pH 7.0). The sodium linoleate substrate was prepared by mixing 70 mg Tween-20 with 70 mg linoleic acid and 4 mL H_2O thoroughly bubbled with argon to remove oxygen. The milky solution was cleared by adding 130 μL 2 N NaOH and filled up to 25 ml with oxygen-free H_2O. The stock solution was stored at -20°C. The kinetic of LOX activity was immediately measured spectrophotometrically at 234 nm with a dwell time of 10 sec. Two hundred μL of extract was mixed with 800 μL KP_i (50 mM pH 7.0) and 8 μL of substrate (linoleic acid). After stabilization of enzyme activity, the reaction kinetic δ234 nm was monitored for 5 min. LOX activity was measured at 25°C and is reported as μkat mg^{-1} total protein, assuming the molecular extinction coefficient of 2.5 x 10^4 M^{-1} cm^{-1} for the conjugated diene product (Axelrod et al. 1981). For each protein extract four technical replicates were analysed. The protein concentration was measured using the Qubit™ protein assay kit (Life Technologies GmbH, Darmstadt, Germany).

Statistical analyses

All measured data were statistically analysed in order to gain insight into the effects of plant genotype and environmental conditions on the release of PIBs. The experiment was designed in a

way that all plants measured from the same sub-chamber (cf. Supplemental Fig. S1a) were handled as technical replicates, i.e. the data were averaged and used as single biological replicate. For each of the IE respectively NE genotypes (IE consisting of WT and PcISPS:GUS/GFP lines; NE consisting of RA1 and RA2 lines) we analysed leaf gas-exchange and PIBs of four independent plant leaves in the CS, PS, CSr and PSr scenario and of eight independent plant leaves in the AC and EC scenario. The experiment was repeated under exactly the same climate and plant conditions to generate four biological replicates (sub-chambers) per treatment (scenario) for the IE and NE genotypes, respectively. Altogether 256 plants were surveyed.

Correlation analyses were performed using Principal Component Analysis (PCA) and Orthogonal Partial Least Square regression (OPLS) (SIMCA-P v13, Umetrics, Umeå, Sweden) between IE or NE genotypes, VOC PIBs area, slopes, enzyme activity and gas exchange parameters (net assimilation, dark respiration, transpiration under light and dark conditions) (all set as X-variables). Thereby, established procedures to analyse MS data were followed as reported previously (Ghirardo et al. 2005; Ghirardo et al. 2012; Kreuzwieser et al. 2014; Vanzo et al. 2014; Velikova et al. 2014, Velikova et al. 2015). For OPLS analysis, seven different Y-variables describing the NE genotypes, the four scenarios (PS, CS, PSr, CSr) and the two controls (AC, EC) were created. Each Y-variable was set to 1 when the sample belonged to the corresponding class and to 0 otherwise. The X-variables were logarithmically transformed, centred and each type of data was block-wise scaled with $1 \ sd^{-1}$. Each calculated significant principal component was validated using "full cross-validation", with 95% confidence level on parameters. The regression model OPLS was tested for significance using CV-ANOVA (Eriksson et al. 2008).

Moreover, two-way ANOVAs were performed in SigmaPlot (v13.0, Systat Software Inc., San Jose, CA, USA) on the means of the measured parameters using the two factors "Scenarios" (AC, EC, PS, CS, PSr, CSr) and "Genotypes" (IE, NE). Tukey post-hoc test followed the ANOVA to pairwise compare particular scenarios and the poplar genotypes. Results were considered significant at $P < 0.05$.

Results and Discussion

In our experiments we could observe PIBs of acetaldehyde, ethanol, isoprene (only in IE plants), hexenal, hexenol and hexenyl acetate isomers. From time to time, small PIBs of two unidentified compounds with sum formulas $C_5H_{11}^+$ (m/z 71.086) and $C_6H_9O_2^+$ (m/z 113.060) were observed. $C_5H_{11}^+$ might be a fragment of a carbonyl deriving from a not yet well established LOX pathway yielding C_5 compounds (Salch et al. 1995, Fall et al. 2001, Jardine et al. 2012, Shen et al. 2014). $C_6H_9O_2^+$ could be a fragment of (E-2)-4-hydroxy-2-hexenal, a substance that was shown to be formed out of Z-3-hexenal in soybean (Takamura & Gardner 1996). Since in our experiments the measured emissions of these unidentified compounds were low, they will not be considered further here.

Figure 1 shows examples of the effect of different treatments (EC, CS, CSr) on plant physiological parameters (assimilation, transpiration, stomatal conductance) and emissions of specific VOCs from IE plants grown under elevated [CO_2]. During HDS most of the VOC PIBs were reduced. In the recovering phase, however, the pattern of the PIBs differed from the control treatment. In the following sections we will show that the amount of VOC emissions following the rapid light-to-dark transitions depended both on the plant genotype and the growth condition. According to their emission rates in the different treatments, they could be subdivided into three different classes linked to different biochemical origins.

Multivariate data analyses separate plant genotypes and treatment effects

Multivariate data analyses revealed a clear pattern of the samples subjected to the different climate scenarios, originating from IE and NE plant genotypes (Fig. 2 and S2). Except for isoprene, all PIBs appeared in plants grown under unstressed conditions (AC+EC scenario), independently from plant genotypes, but they were mostly suppressed in plants grown under CS and PS scenarios. This is illustrated in Fig. 2: the first principal component (PC1) of PCA separates CS and PS samples (right

side of the loading plot in Fig. 2a) from samples grown in the AC, EC, CSr and PSr climate scenarios; VOC PIBs are located on the opposite side (negative correlation) of the loading plot (Fig. 2b). In contrast to IE plants, the NE genotypes were affected differently by the CS and PS treatments. This effect is illustrated by the clear treatment-dependent clustering within the NE samples (Fig. 2a). The PIBs originating from samples under CS and PS decreased in concert with the physiological parameters net assimilation and transpiration rates, but also with methanol emission rates (under light) and *in-vitro* LOX enzyme activities.

We employed OPLS analysis to further investigate which parameters correlate strongest with the plant genotypes or the different climatic conditions (Fig. S2 and S3). The distinction between the four different plant genotypes mainly originated from their ability to either emit or not emit isoprene under constant light and was independent of treatment, as indicated by the high negative correlation coefficient (see Fig. S3a). The genotype effect was clearly revealed by the second principal component (PC2) in both PCA and OPLS (Fig. 2 and S2, respectively) and was related to constitutive isoprene emission rates and partially to PIBs of isoprene and dark respiration (denoted as 'IS', 'b69' and '–A' respectively, in both Fig. 2b and S2; see also correlation coefficients in Fig. S3a). This is the reason why we pooled together WT and PcISPS:GUS/GFP genotypes (IE) as well as RA1 and RA2 plants (NE) and considered for further analysis only the IE and NE class.

Overall, the OPLS model was very reliable as seen by the high numerical value of $Q^2(Y) = 94.4\%$. Other performance indicators were: $R^2(X) = 80\%$, $R^2 = 36\%$, $R^2(Y) = 67\%$ using four PC. Furthermore, we used the CV-ANOVA, based on cross-validated predictive residuals (Eriksson et al. 2008) to test the significance of the OPLS models created, and found that the model was highly significant to describe genotype and treatments, resulting in the following P-values: $<1e^{-14}$ (describing NE/IE genotypes), $4.9e^{-9}$ (AC), $2.0e^{-7}$ (EC), $2.7e^{-13}$ (PS), $2.7e^{-14}$ (CS), $3.9e^{-10}$ (CSr). Only the model explaining samples of the PSr scenario was not found significant (P=0.36).

Heat and drought spells had only little effect on post illumination bursts of isoprene

In poplar plants, isoprene is the most abundant VOC emitted from leaves; also other VOCs can be emitted significantly in a constitutive manner with leaf age dependent emission potentials (Ghirardo et al. 2011). In the transgenic poplar plants used in our experiments, knocking down of isoprene synthase (ISPS) causes the almost complete suppression of isoprene biosynthesis (Behnke et al. 2007). This had also impact on the PIBs of isoprene.

In experiments with IE plants, switching off the light caused the well-known PIBs of isoprene (cf. Fig. 1). During these bursts, approximately 0.04 to 0.06 nmol cm^{-2} of isoprene was emitted, independently from the plant treatment (see Fig. 3a; P > 0.05, see Supplemental table S1). Only in the CS scenario was the absolute amount of isoprene emitted as PIB slightly lower, although not statistically different. The observation that the PIB isoprene emission, like constitutive isoprene emission, is unaffected by HDS, supports the current knowledge that in both cases the emitted isoprene molecules derive from the same substrate. As mentioned earlier, the PIB of isoprene originates from a pool of MEP pathway intermediates after the light-dependent HMBDP synthase enzyme has switched to NADPH as electron donor and newly available DMADP is quickly converted into isoprene by ISPS (Li & Sharkey 2013).

Consistently, the lack of ISPS in NE plants resulted in a suppression of the typical isoprene PIBs, although in NE plants the chloroplastic DMADP pool is much higher than in IE plants (Ghirardo et al. 2014). However, from time to time we detected some tiny PIBs at the mass-to-charge ratio of isoprene (m/z 69.070) in NE plants recovering from HDS. It is unclear whether these signals were caused by isoprene or by a fragment of some interfering C$_5$ compound (Salch et al. 1995, Fall et al. 2001, Jardine et al. 2012, Shen et al. 2014). The latter could be supported by an apparent correlation of the appearance of these bursts with PIBs of an unidentified C$_5$ compound at m/z 71.086 about half a minute earlier. If these occasional early burst signals at m/z 69.070 appeared also in IE plants, they could likely not be resolved from the high isoprene signals slowly decaying after quitting the leaf

illumination (cf. Fig. 1). While the maximum of regular isoprene PIBs appeared after a mean time span of 729 s (minimum ~ 400 s, maximum ~ 1294 s), the PIBs of NE plants appeared much faster after 102 s (minimum ~ 60 s, maximum ~ 193 s), see Fig. 4. Due to these facts, in such cases the PIB values were neglected in the actual analysis of isoprene PIBs (and Fig. 3a).

Acetaldehyde post illumination bursts as a result of DXS activity?

Acetaldehyde emissions following light-to-dark transitions have been observed in several plant species (see e.g. Holzinger et al. 2000, Karl et al. 2002, Graus et al. 2004, Ghirardo et al. 2011, Jardine et al. 2012). In *Quercus Ilex L.* the PIBs of acetaldehyde were accompanied by ethanol PIBs (Holzinger et al. 2000), while in sycamore, aspen, cottonwood and maple leaves no concomitant ethanol emissions were observed (Karl et al. 2002). Jardine et al (2012) detected also PIBs of acetic acid and acetone, which were thought to derive from the same synthetic pathway (see also Jardine et al. 2010). This variation in the pattern of C_2 compound emissions is indicative for a high complexity of the involved synthesis pathways and the impact of the plants' biochemical status on the emission.

In our experiments the absolute amounts of C_2 compound (acetaldehyde+ethanol) emissions during PIBs were lower in NE than in IE plants (P < 0.001) and they were almost totally suppressed in the CS and PS scenarios (cf. Table 1 and Fig. 3b). This is also depicted by the negative OPLS correlation coefficients of acetaldehyde and ethanol in these scenarios (Fig. S3d+e). In plants recovering from HDS, the emissions as PIBs of the C_2 compounds were significantly lower than in the corresponding control treatments (P < 0.007 for acetaldehyde, P < 0.09 for ethanol).

Three sources of post illumination acetaldehyde emission can be imagined: (i) reaction of ADH to convert ethanol to acetaldehyde, (ii) action of pyruvate decarboxylase in the cytosol, and (iii) release during the complex kinetics of deoxyxylulose phosphate synthase.

The peaks of the ethanol PIBs appeared always after those of acetaldehyde (mean time difference of burst peaks: 58±18 s, see Fig. 4). The obvious correlation (R^2=0.98) between acetaldehyde and ethanol PIBs (cf. Table 1) rather supports the reverse reaction of the ADH, in which ethanol is formed out of acetaldehyde.

When the light is abruptly turned off, CO_2 will continue to be fixed until all of the ribulose-1,5-bisphosphate (RuBP) in the Calvin-Benson-Bassham cycle (CBB) is consumed (Laisk et al. 1984). However, reducing power in the form of NADPH is not available, resulting in a large increase in phosphoglyceric acid (PGA) and pyruvate immediately after a light to dark transient. This pyruvate could be consumed by cytosolic PDC and form acetaldehyde in what Karl et al. (2002) called the "pyruvate overflow mechanism" and Jardine et al (2012) the "PDH bypass pathway".

The third potential source of acetaldehyde is 1-deoxy-D-xylulose-5-phosphate synthase (DXS). DXS is responsible for the formation of 1-deoxy-D-xylulose-5-phosphate (DXP) from pyruvate and glyceraldehyde-3-phosphate (GAP) in the first step of the MEP pathway (Ghirardo et al. 2010). DXS first forms a decarboxylated thiamine diphosphate (ThDP) – pyruvate complex to make hydroxyethyl ThDP. This step is the same as the first step of PDC. In the case of PDC, the hydroxyethyl ThDP is hydrolysed to acetaldehyde and ThDP. It is worth future research into whether the post illumination stromal environment causes DXS to act as a PDC for a short time.

Another possibility is that DXS could reverse part of the reaction sequence to liberate GAP and hydroxyethyl-ThDP or just acetaldehyde. Release of GAP from DMADP has been observed (A. Banerjee, T.D. Sharkey, unpublished).

This proposed mechanism is coherent with findings of Karl et al. (2002). In $^{13}CO_2$ labelling experiments with cottonwood leaves, after about 100 min of $^{13}CO_2$ fumigation in light they found comparable labelling of both isoprene (78 %) and acetaldehyde (60%).

Previous observations of enhanced acetaldehyde emissions when using PDH (Graus et al. 2004) or pyruvate transport inhibitors (Karl et al. 2002) and the observed dependence of the acetaldehyde PIBs on CO_2 availability and assimilation rates (Jardine et al. 2012) are consistent with the proposed role of DXS in the acetaldehyde formation involving pyruvate, too. Eventually, acetaldehyde can be further processed by ALDH to acetic acid, which has been observed following PIBs of acetaldehyde (Jardine et al. 2012).

A role for DXS in the acetaldehyde burst is also consistent with data presented in Fig. 3 and Fig. S3a, showing lower acetaldehyde PIBs in NE than in IE plants. It is known that high DMADP levels in chloroplasts act as feedback regulator of the MEP pathway, by inhibiting the activities of DXS (Wolfertz et al. 2004, Banerjee et al. 2013, Ghirardo et al. 2014). In NE plants, the suppression of ISPS leads to an accumulation of chloroplastic DMADP, which causes a strong down regulation of the DXS activity (Ghirardo et al. 2014) and DXS protein levels, resulting in a reduced metabolic C-flux throughout the MEP pathway. Taken together, the lower DXS activities and protein levels of NE compared to IE plants (Ghirardo et al. 2014) and the proposed change in DXS catalytic properties might be the reason of the low PIBs of acetaldehyde from NE leaves. Moreover, the MEP pathway is ubiquitous in all plant species, which explains why the PIB emissions of acetaldehyde are detected independently from the trait to emit isoprene (Brilli et al. 2011).

Nonetheless, we cannot exclude that the differences between IE and NE plants derive from comprehensive changes in metabolite concentrations (Way et al. 2013) and metabolic fluxes (Ghirardo et al., 2014), rearrangements of enzymatic and functional protein contents (Velikova et al. 2014) or changes in lipid composition (Velikova et al. 2015). Moreover, this proposed explanation for the differences between acetaldehyde emissions of IE and NE genotypes does not fully explain why the PIBs were suppressed in drought and temperature stressed plants (CS and PS scenario), although the constitutive emission of isoprene, an end product in the MEP pathway, in IE plants is unaffected

by HDS. A possible explanation for this effect can be an up-regulation of ADH and ALDH genes during HDS, as has been reported for Arabidopsis (Seki et al. 2002).

Reduced LOX activity in HDS-stressed plants suppressed PIBs of green leaf volatiles

In unstressed plants (AC, EC) and plants recovering from HDS (CSr, PSr), switching off the light caused a strong transient release of different volatile C_6 compounds (GLVs). The GLVs could be associated with their precursor α-linolenic acid (C18:3), the most abundant fatty acid in lipids composing the chloroplast membranes of grey poplar (Velikova et al. 2015). This fact allowed to infer the isomeric structure of the GLVs emitted.

As examples for GLV emissions we show the amount of the isomers E-2-hexenal / Z-3-hexenal and Z-3-hexenol emitted as PIBs under the different climate scenarios (Fig. 3c+d). Generally, the PIBs of the C_6 compounds showed behaviour similar to the PIB emissions of the C_2 compounds in terms of the $[CO_2]$ and HDS effect. Elevated growth $[CO_2]$ influenced the PIBs of GLVs in NE plants only, when compared to AC (see Fig. 3c+d). Overall, PIBs of GLVs negatively correlated to NE plants (Fig. S3a). Apart from the EC scenario, NE genotypes generally showed lower PIBs of GLVs (cf. Table 1 and Fig. 3) compared with IE genotypes.

Additional biochemical analyses revealed that the *in-vitro* LOX protein activities were reduced in protein extracts from NE compared to IE (Fig. 5 and Fig. S3b) and correlated well with NE plants (Fig. S3a). Thus, the lower amount of GLVs released from NE genotypes during light-to-dark transitions appears to be a consequence of both the reduced substrate availability (α-linolenic acid for the LOX enzymes, see Velikova et al. (2015)) and the lower LOX enzyme activities.

The PIBs of GLVs were almost completely suppressed during HDS (cf. Fig. 3), independently from genotype. Previous studies have shown rather an increase in GLV emissions during heat stress, although not in the course of light-to-dark transitions (Gouinguené + Turlings 2002, Loreto et al.

2006, Hartikainen et al. 2009, Behnke et al. 2013). Under light, neither IE nor NE plants showed any GLV emissions under the PS and CS treatments (Vanzo et al., 2015, supplemental data), indicating that the stress exposure was not detrimental for membranes. The applied eustress is per definition a mild, stimulating stress, strengthening plant resistance (Lichtenthaler, 1996). It can be speculated that the stress, plants experienced in the studies cited above, exceeded the plant's limit of tolerance (= resistance minimum), leading to membrane damage and consequently GLV emissions.

In our experiments the suppressed GLV PIBs correlated with a notable reduction of *in-vitro* LOX activities found from leaf extracts (see Fig. 2b and Fig. 5), which was more pronounced in chronically-stressed plants than in periodically-stressed ones. However, even in stressed plants the apparent LOX activity did not drop to zero, indicating that additional mechanisms might have been involved in the suppression of *in-vivo* LOX activity following the light-to-dark transition. Earlier studies revealed altered portions of saturated and unsaturated fatty acids in response to drought. For example, drought stress decreased the ratio of α-linolenic (C18:3) to linoleic acid (C18:2) in *Carthamus tinctorius* (Hamrouni et al. 2001) and caused a reduction in the abundance of C18:3 fatty acids as well as a complete disappearance of palmitoleic acid (C16:1) in *Salvia officinalis* leaves (Bettaieb et al. 2009). Also in Bermuda grass (*Cynodon dactylon*) the portion of unsaturated fatty acids decreased during drought stress (Zhong et al. 2011). It is likely that the reduction in unsaturated fatty acids in these examples also would cause a reduction of the PIBs of GLVs when analysed during drought stress. Another possible explanation for reduced GLV PIBs in HDS plants is the effect of elevated abscisic acid (ABA) levels. Drought stress leads to increased ABA transport from the roots to the leaves (e.g. Wilkinson & Davies 2002). It has been shown that ABA has a strong inhibitory effect on LOX, while it is increasing the antioxidant capacity in *Orthosiphon stamineus* (Ibrahim & Jaafar 2013). Both effects might result in a reduced formation of GLVs as we have seen herein. The strong suppression of GLV, but also acetaldehyde PIBs under drought and temperature stress may therefore be used as non-invasive marker for plant phenotyping (Niederbacher et al. 2015).

Apparently, in our experiments the HDS had no remarkable effect on the reaction speed during the formation of the LOX products (see Fig. 4). Only the end product Z-3-hexenyl acetate seems to have been formed with a certain delay in CS/CSr and PS/PSr plants compared to control plants.

A remarkable difference between the PIBs of GLVs and acetaldehyde/ethanol became evident in plants recovering from HDS (CSr and PSr scenarios). The PIBs of GLVs were markedly more pronounced in CSr and PSr plants compared to control plants, while the PIB emissions of C_2 compounds were reduced (see Table 1 and previous section). This indicates that both types of PIBs were biochemically independent, either deriving from different substrate pools or requiring different enzymatic formation processes (see e.g. Graus et al. 2004, Jardine et al. 2012). Moreover, the differences in the PIBs of acetaldehyde and Z-3-hexenyl acetate (reduced vs. enhanced emissions) in the CSr and PSr scenarios indicate that these are not directly linked wire acetyl CoA, unlike Jardine et al. (2012) concluded from their ^{13}C labelling experiments.

We hypothesize that enhanced GLV PIBs after recovery might have been a result of altered membrane composition during HDS and an increase of LOX activity (Fig. 5 and Supplemental table S2). During stress events plants remodel membrane fluidity (see above) and also release large amounts of α-linolenic acid from membrane lipids (Upchurch 2008). In plants recovering from HDS, ABA levels are recovering to normal values faster than those of the free lipids. Also the fatty acid composition might change back to more unsaturated ones. Consequently, in CSr and PSr plants higher enzyme activity of 13-LOX, most obvious of IE plants (see Fig. 5), and substrate pools for the GLV formation were available. These facts eventually resulted in higher GLV PIBs in plants recovering from HDS.

Conclusion

Our experiments showed that PIBs of acetaldehyde, ethanol and GLVs are potential markers for the heat and drought stress status of poplar plants. Under physiological stress conditions, these PIBs almost disappeared. While PIBs of acetaldehyde were lower in plants recovering from HDS in respect to the corresponding control plants, PIBs of GLVs were enhanced. This observation supports the suggestion, that acetaldehyde and GLV PIBs are not directly linked biochemically.

Reduced acetaldehyde PIBs in NE plants were potentially a result of the feedback inhibition of DXS in the MEP pathway in plants lacking ISPS. Analysing the kinetic properties of DXS to release acetaldehyde from hydroxyethyl-ThDP under biochemical conditions experienced just after light-to-dark transition might help clarifying the origin of the PIB acetaldehyde emissions in plants.

Our results demonstrated that in grey poplar analysing PIBs of GLVs might be useful as a non-invasive phenotypic marker of stress-induced changes in free fatty acids or fatty acid composition of chloroplast membranes and *in planta* LOX activity under given environmental conditions. Based on the present data it might be promising to test in other plant species whether the reduction of PIBs of C_2 compounds and GLVs is a general phenomenon and is applicable as non-invasive phenotypic marker, quantifying the susceptibility of genotypes under drought and heat (eu)stress.

Conflict of interest

Acknowledgments

References

Axelrod B., Cheesbrough T.M. & Laakso S. (1981) Lipoxygenase from soybeans. EC 1.13.11.12 Linoleate:oxygen oxidoreductase. *Methods in Enzymology* **71**, 441-451.

Banerjee A., Wu Y., Banerjee R., Li Y., Yan H. & Sharkey T.D. (2013) Feedback inhibition of deoxy-D-xylulose-5-phosphate synthase regulates the methylerythritol4-phosphate pathway. *Journal of Biological Chemistry* **288**, 16926-16936.

Behnke K., Ehlting B., Teuber M., Bauerfeind M., Louis S., Hänsch R., ..., Schnitzler J.P. (2007) Transgenic, non-isoprene emitting poplars don't like it hot. *The Plant Journal* **51**, 485-499.

Behnke K., Ghirardo A., Janz D., Kanawati B., Esperschütz J., Zimmer I., ..., Rosenkranz M. (2013) Isoprene function in two contrasting poplars under salt and sunflecks. *Tree Physiology* **33**, 562-578.

Bethmann B., Simonis W. & Schonknecht G. (1998) Light-induced changes of cytosolic pH in *Eremosphaera viridis*: recordings and kinetic analysis. *Journal of Experimental Botany* **49**, 1129-1137.

Bettaieb I.N., Zakhama W., Wannes M., Kchouk M.E. & Marzouk B. (2009) Water deficit effects on *Salvia officinalis* fatty acids and essential oils composition. *Scientia Horticulturae* **120**, 271–275.

Boubekeur S., Camougrand N., Bunoust O., Rigoulet M. & Guérin B. (2001) Participation of acetaldehyde dehydrogenases in ethanol and pyruvate metabolism of the yeast Saccharomyces cerevisiae. *European Journal of Biochemistry* **268**, 5057-5065.

Brilli F., Ruuskanen T.M., Schnitzhofer R., Müller M., Breitenlechner M., Bittner V., ..., Hansel A. (2011) Detection of plant volatiles after leaf wounding and darkening by proton transfer reaction "time-of-flight" mass spectrometry (PTR-TOF). *PloS ONE* **6**, e20419.

Cinege G., Louis S., Hänsch R. & Schnitzler J.P. (2009) Regulation of isoprene synthase promoter by environmental and internal factors. *Plant Molecular Biology* **69**, 593-604.

D'Auria J.C., Pichersky E., Schaub A., Hansel A. & Gershenzon J. (2007) Characterization of a BAHD acyltransferase responsible for producing the green leaf volatile (Z)-3-hexen-1-yl acetate in Arabidopsis thaliana. *Plant Journal* **49**, 194-207.

DeNiro M. & Epstein S. (1977) Mechanism of carbon isotope fractionation associated with lipid synthesis. *Science* **197**, 261-263.

Eriksson L., Trygg J. & Wold S. (2008) CV-ANOVA for significance testing of PLS and OPLS models. *Journal of Chemometrics* **22**, 594-600.

Fall R., Karl T., Hansel A., Jordan A. & Lindinger W. (1999) Volatile organic compounds emitted after leaf wounding: On-line analysis by proton-transfer reaction mass spectrometry. *Journal of Geophysical Research* **104**, 15963-15974.

Fall R., Karl T., Jordan A. & Lindinger W. (2001) Biogenic C5 VOCs: release from leaves after freeze– thaw wounding and occurrence in air at a high mountain observatory. *Atmospheric Environment* **35**, 3905-3916.

Ghirardo A., Sørensen H.A., Petersen M., Jacobsen S. & Søndergaard I. (2005) Early prediction of wheat quality: Analysis during grain development using mass spectrometry and multivariate data analysis. *Rapid Communications in Mass Spectrometry* **19**, 525-532.

Ghirardo A., Gutknecht J., Zimmer I., Brüggemann N. & Schnitzler J.P. (2011) Biogenic volatile organic compound and respiratory CO_2 emissions after ^{13}C-labeling: Online tracing of C translocation dynamics in poplar plants. *PLoS ONE* **6**, 2-5.

Ghirardo A., Heller W., Fladung M., Schnitzler J.P. & Schroeder H. (2012) Function of defensive volatiles in pedunculate oak (*Quercus robur*) is tricked by the moth *Tortrix viridana*. *Plant, Cell and Environment* **35**, 2192-2207.

Ghirardo A., Wright L.P., Bi Z., Rosenkranz M., Pulido P., Rodriguez-Concepción M., …, Schnitzler J.P. (2014) Metabolic flux analysis of plastidic isoprenoid biosynthesis in poplar leaves emitting and nonemitting isoprene. *Plant Physiology* **165**, 37-51.

Gouinguené S.P. & Turlings T.C.J. (2002) The Effects of Abiotic Factors on Induced Volatile Emissions in Corn Plants. *Plant Physiology* **129**, 1296-1307.

Graus M., Schnitzler J.P., Hansel A., Cojocariu C., Rennenberg H., Wisthaler A. & Kreuzwieser J. (2004) Transient release of oxygenated volatile organic compounds during light-dark transitions in Grey poplar leaves. *Plant Physiology* **135**, 1967-1975.

Graus M., Müller M. & Hansel A. (2010) High resolution PTR-TOF: quantification and formula confirmation of VOC in real time. *Journal of the American Society for Mass Spectrometry* **21**, 1037-1044.

Guenther A.B., Jiang X., Heald C.L., Sakulyanontvittaya T., Duhl T., EmmonsL.K. & Wang X. (2012) The Model of Emissions of Gases and Aerosols from Nature version 2.1 (MEGAN2.1): an extended and updated framework for modeling biogenic emissions. *Geoscientific Model Development* **5**, 1471-1492.

Hamrouni I., Salah H. & Marzouk B. (2001) Effects of water-deficit on lipids of safflower aerial parts. *Phytochemistry* **58**, 277–280.

Harry D.E. & Kimmerer T.W. (1991) Molecular genetics and physiology of alcohol dehydrogenase in woody plants. *Forest Ecology and Management* **43**, 251-272.

Hartikainen K., Nerg A.-M., Kivimäenpää M., Kontunen-Soppela S., Mäenpää M., Oksanen E., …, Holopainen T. (2009) Emissions of volatile organic compounds and leaf structural characteristics of European aspen (Populus tremula) grown under elevated ozone and temperature. *Tree Physiology* **29**, 1163-1173.

Hatanaka A. (1993) The biogeneration of green odour by green leaves. *Phytochemistry* **34**, 1201-1218.

Hayward S., Tani A., Owen S.M. & Hewitt C.N. (2004) Online analysis of volatile organic compound emissions from Sitka spruce (*Picea sitchensis*). *Tree Physiology* **24**, 721-728.

Hobbie E.A. & Werner R.A. (2004) Intramolecular, compound-specific, and bulk carbon isotope patterns in C_3 and C_4 plants: a review and synthesis. *New Phytologist* **161**, 371-385.

Holopainen J.K & Gershenzon J. (2010) Multiple stress factors and the emission of plant VOCs. *Trends in Plant Science* **15**, 176-184.

Holzinger R., Sandoval-Soto L., Rottenberger S., Crutzen P.J. & Kesselmeier J. (2000) Emissions of volatile organic compounds from *Quercus ilex* L. measured by Proton Transfer Reaction Mass Spectrometry under different environmental conditions. *Journal of Geophysical Research* **105**, 20573.

Ibrahim M.H. & Jaafar H.Z.E. (2013) Abscisic acid induced changes in production of primary and secondary metabolites, photosynthetic capacity, antioxidant capability, antioxidant enzymes and lipoxygenase inhibitory activity of *Orthosiphon stamineus* Benth. *Molecules* **18**, 7957-7976.

Jardine K.J., Karl T., Lerdau M., Harley P., Guenther A.B. & Mak J.E. (2009) Carbon isotope analysis of acetaldehyde emitted from leaves following mechanical stress and anoxia. *Plant Biology* **11**, 591-597.

Jardine K.J., Sommer E.D., Saleska S.R., Huxman T.E., Harley P.C. & Abrell L. (2010) Gas phase measurements of pyruvic acid and its volatile metabolites. *Environmental Science and Technology* **44**, 2454-2460.

Jardine K., Barron-Gafford G.A., Norman J.P., Abrell L., Monson R.K., Meyers K.T.,…,Huxmann T.E. (2012) Green leaf volatiles and oxygenated metabolite emission bursts from mesquite branches following light–dark transitions. *Photosynthesis Research* **113**, 321-333.

Karl T., Curtis A.J., Rosenstiel T.N., Monson R.K. & Fall R. (2002) Transient releases of acetaldehyde from tree leaves - products of a pyruvate overflow mechanism? *Plant, Cell and Environment* **25**, 1121-1131.

Keppler F., Kalin R.M., Harper D.B., McRoberts W.C. & Hamilton J.T.G. (2004) Carbon isotope anomaly in the major plant C1 pool and its global biogeochemical implications. *Biogeosciences* **1**, 123-131.

Kesselmeier J. & Staudt M. (1999) Biogenic Volatile Organic Compounds (VOC): An Overview on Emission, Physiology and Ecology. *Journal of Atmospheric Chemistry* **33**, 23-88.

Kimmerer T.W. & MacDonald R.C. (1987) Acetaldehyde and Ethanol Biosynthesis in Leaves of Plants. *Plant Physiology* **84**, 1204-1209.

Koch E., Meier B.M., Eiben H.G. & Slusarenko A. (1992) A Lipoxygenase from Leaves of Tomato (*Lycopersicon esculentum* Mill.) Is Induced in Response to Plant Pathogenic Pseudomonads. *Plant Physiology* **99**, 571-576.

Kreuzwieser J., Scheerer U. & Rennenberg H. (1999) Metabolic origin of acetaldehyde emitted by poplar (Populus tremula x P. alba) trees. *Journal of Experimental Botany* **50**, 757-765.

Kreuzwieser J., Kuhnemann F., Martis A., Rennenberg H. & Urban W. (2000) Diurnal pattern of acetaldehyde emission by flooded poplar trees. *Physiologia Plantarum* **108**, 79-86.

Kreuzwieser J., Harren F.J.M., Laarhoven L.J.J., Boamfa I., te Lintel-Hekkert S., Scheerer U., ..., Rennenberg H. (2001) Acetaldehyde emission by the leaves of trees - correlation with physiological and environmental parameters. *Physiologia Plantarum* **113**, 41-49.

Kreuzwieser J., Scheerer U., Kruse J., Burzlaff T., Honsel A., Alfarraj S., ..., Rennenberg H. (2014) The Venus flytrap attracts insects by the release of volatile organic compounds. *Journal of Experimental Botany* **65**, 755-766.

Laisk A., Kiirats O. & Oja V. (1984) Assimilatory Power (Postillumination CO_2 Uptake) in Leaves: Measurement, Environmental Dependencies, and Kinetic Properties. *Plant Physiology* **76**, 723-729.

Li Z., Ratliff E.A. & Sharkey T.D. (2011) Effect of temperature on postillumination isoprene emission in oak and poplar. *Plant Physiology* **155**, 1037-46.

Li Z. & Sharkey T.D. (2013) Metabolic profiling of the methylerythritol phosphate pathway reveals the source of post-illumination isoprene burst from leaves. *Plant, Cell and Environment* **36**, 429-37.

Lichtenthaler H.K. (1996) Vegetation stress: An introduction to the stress concept in plants. *Journal of Plant Physiology* **148,** 4-14.

Loreto F., Barta C., Brilli F. & Nogues I. (2006) On the induction of volatile organic compound emissions by plants as consequence of wounding or fluctuations of light and temperature. *Plant, Cell and Environment* **29**, 1820-1828.

Loreto F. & Schnitzler J.-P. (2010) Abiotic stresses and induced BVOCs. *Trends in Plant Science* **15**, 154-166.

Monson R.K., Hills A.J., Zimmerman P.R. & Fall R.R. (1991) Studies of the relationship between isoprene emission rate and CO_2 or photon-flux density using a real-time isoprene analyser. *Plant, Cell and Environment* **14**, 517-523.

Müller M., Mikoviny T., Jud W., D'Anna B. & Wisthaler A. (2013) A new software tool for the analysis of high resolution PTR-TOF mass spectra. *Chemometrics and Intelligent Laboratory Systems* **127**, 158-165.

Niederbacher B., Winkler J.B. & Schnitzler J.-P. (2015) Volatile organic compounds as non-invasive markers for plant phenotyping. *Journal of Experimental Botany,* **66**, 5403-5416.

Park R. & Epstein S. (1961) Metabolic fractionation of C13 & C12 in plants. *Plant Physiology* **36**, 133-138.

Salch Y.P., Grove M.J., Takamura H. & Gardner H.W. (1995) Characterization of a C-5,13-Cleaving Enzyme of 13(S)-Hydroperoxide of Linolenic Acid by Soybean Seed. *Plant Physiology* **108**, 1211-1218.

Scala A., Allmann S., Mirabella R., Haring M.A. & Schuurink R.C. (2013) Green leaf volatiles: a plant's multifunctional weapon against herbivores and pathogens. *International Journal of Molecular Sciences* **14**, 17781-17811.

Seemann M. & Rohmer M. (2007) Isoprenoid biosynthesis via the methylerythritol phosphate pathway: GcpE and LytB, two novel iron-sulphur proteins. *Comptes Rendus Chimie* **10**, 748-755.

Seki M., Narusaka M., Ishida J., Nanjo T., Fujita M., Oono Y., ..., Shinozaki K. (2002) Monitoring the expression profiles of 7000 Arabidopsis genes under drought, cold and high-salinity stresses using a full-length cDNA microarray. *The Plant Journal* **31**, 279-292.

Shen J., Tieman D., Jones J.B., Taylor M.G., Schmelz E., Huffaker A., ..., Klee H.J. (2014) A 13-lipoxygenase, TomloxC, is essential for synthesis of C5 flavour volatiles in tomato. *Journal of Experimental Botany* **65**, 419-428.

Takamura H. & Gardner H.W. (1996) Oxygenation of (3Z)-alkenal to (2E)-4-hydroxy-2-alkenal in soybean seed (*Glycine max* L.). *Biochimica et Biophysica Acta (BBA) - Lipids and Lipid Metabolism* **1303**, 83-91.

Upchurch R.G. (2008) Fatty acid unsaturation, mobilization, and regulation in the response of plants to stress. *Biotechnology Letters* **30**, 967-977.

Vanzo E., Ghirardo A., Merl-Pham J., Lindermayr C., Heller W., Hauck S.M., …, Schnitzler J.P. (2014) S-Nitroso-Proteome in Poplar Leaves in Response to Acute Ozone Stress. *PLoS ONE* **9**, e106886.

Vanzo E., Jud W., Li Z., Albert A., Domagalska M.A., Ghirardo A., …, Schnitzler J.P. (2015) Facing the future - Effects of short-term climate extremes on isoprene-emitting and non-emitting poplar. *Plant Physiology,* **169**, 560-575.

Velikova V., Ghirardo A., Vanzo E., Merl J., Hauck S.M. & Schnitzler J.P. (2014) Genetic manipulation of isoprene emissions in poplar plants remodels the chloroplast proteome. *Journal of Proteome Research* **13**, 2005-2018.

Velikova V., Müller C., Ghirardo A., Rock T.M., Aichler M., Walch A., ..., Schnitzler J.P. (2015) Knocking down of isoprene emission modifies the lipid matrix of thylakoid membranes and influences the chloroplast ultrastructure in poplar. *Plant Physiology* **168**, 859-870.

Way D.A., Ghirardo A., Kanawati B., Esperschütz J., Monson R.K., Jackson R.B., …, Schnitzler J.P. (2013) Increasing atmospheric CO_2 reduces metabolic and physiological differences between isoprene- and non-isoprene-emitting poplars. *The New Phytologist* **200**, 534-546.

Wei Y., Lin M., Oliver J.D. & Schnable P.S. (2009) The roles of aldehyde dehydrogenases (ALDHs) in the PDH bypass of Arabidopsis. *BMC Biochemistry* **10**:7.

Wilkinson S. & Davies W.J. (2002) ABA-based chemical signalling: the coordination of responses to stress in plants. *Plant, Cell and Environment* **25**, 195-210.

Wolfertz M., Sharkey T.D., Boland W. & Kühnemann F. (2004) Rapid regulation of the methylerythritol 4-phosphate pathway during isoprene synthesis. *Plant Physiology* **135**, 1939-1945.

Zhong D., Du H. & Wang Z.h. (2011) Genotypic variation in fatty acid composition and unsaturation levels in Bermuda grass associated with leaf dehydration tolerance. *Journal of the American Society for Horticultural Science* **136**, 35–40.

Table 1: Genotype and climate scenario specific post illumination VOC emissions in poplar. Values are means of n=4 biological replicates (± s.e.) and denote the area under the post illumination bursts, normalized to the leaf area. Since the PTR-ToF-MS has no isomeric separation capability and signals at several mass-to-charge ratios (m/z) correspond to fragments of more than one GLV, assigning sensitivities to certain ion signals is difficult. The emissions are therefore given in normalized counts per second per cm^2 leaf area [ncps $cm^{-2}_{Leaf\ area}$]. Refer to the main text for the assignment of molecules to m/z ratios. Statistical results are given in Supplemental table S1. Abbreviations used: IE: isoprene emitter, NE: isoprene non-emitter, AC: ambient control, EC: elevated control, CS: chronic stress, PS: periodic stress, CSr: chronic stress recovery, PSr: periodic stress recovery.

| Genotype	Scenario	m/z45	m/z47	m/z57	m/z69	m/z71	m/z81	m/z83	m/z99	m/z101	m/z113	m/z143
IE	AC	26842±5345	218±46	154±76	681±259	45±21	3058±1422	2364±436	1616±743	46±12	9±5	66±11
NE	AC	8459±4639	82±36	44±26	0±0	12±9	918±607	1213±511	474±309	17±9	2±2	33±13
IE	EC	25195±1318	246±31	124±45	750±385	27±4	2034±319	3266±881	1124±207	54±18	3±1	87±27
NE	EC	14635±1193	140±14	122±30	0±0	28±6	2324±438	2968±611	1237±244	52±11	3±1	93±16
IE	PS	33±33	0±0	12±7	803±278	0±0	114±56	262±129	66±31	0±0	0±0	0±0
NE	PS	0±0	0±0	0±0	0±0	0±0	0±0	0±0	0±0	0±0	0±0	0±0
IE	CS	1423±1004	14±9	62±16	605±176	8±8	878±449	1332±346	481±209	16±9	1±1	14±14
NE	CS	0±0	0±0	0±0	0±0	0±0	0±0	0±0	0±0	0±0	0±0	0±0
IE	PSr	12090±4163	156±27	948±315	904±525	93±40	5913±2322	5696±958	3960±1180	136±21	13±8	112±6
NE	PSr	6965±3802	83±49	364±202	0±0	57±33	3597±2029	3830±1721	2100±1167	74±38	11±6	83±36
IE	CSr	5606±1897	79±23	874±159	644±272	181±51	11048±2911	10296±543	6304±1368	265±39	25±11	210±25
NE	CSr	2405±1318	36±21	393±161	0±0	107±55	6747±3182	9200±3177	3561±1585	181±62	17±10	187±49
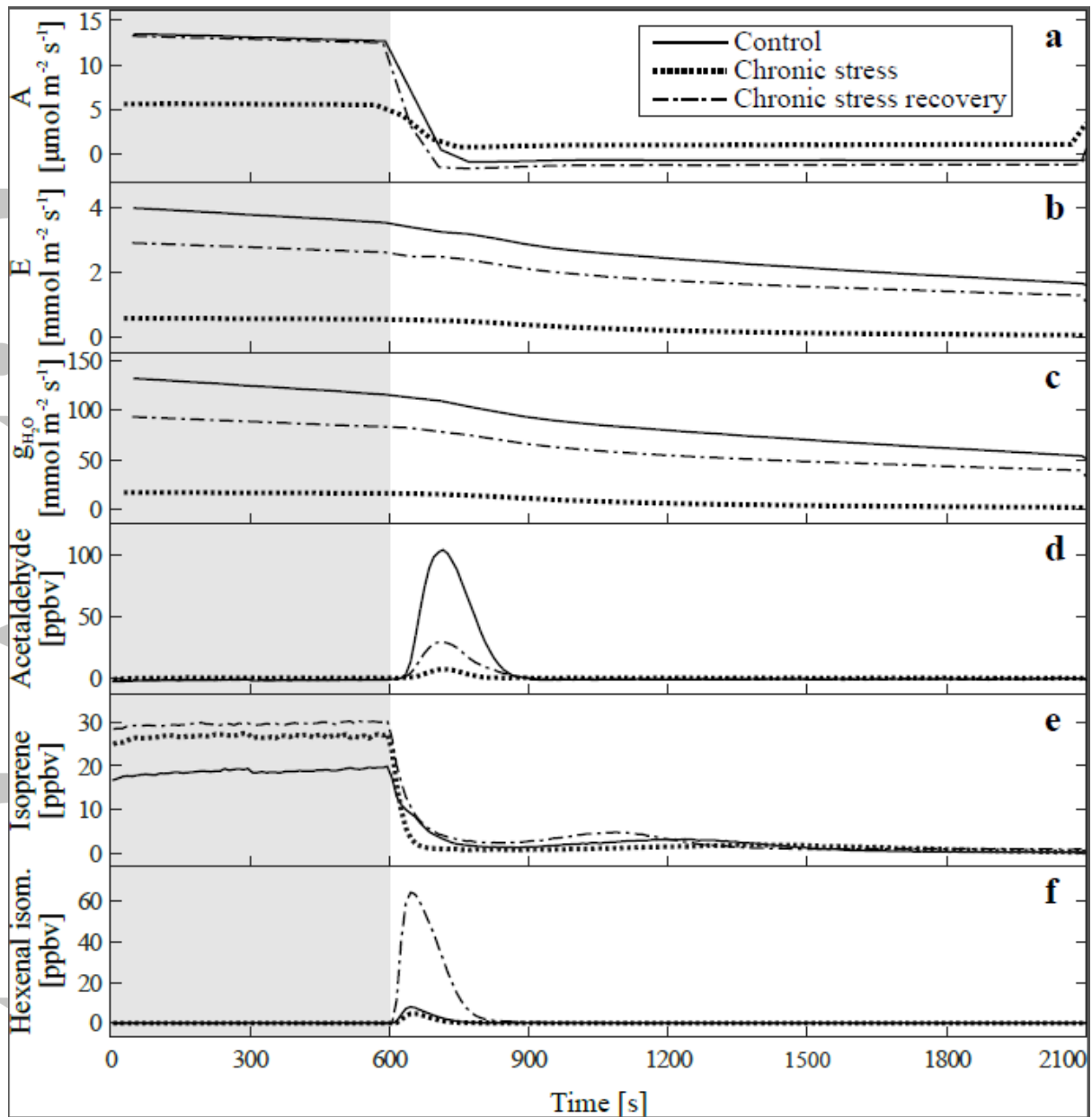
Figure 1: Gas-exchange parameters (assimilation rate A (**a**), transpiration rate E (**b**) and water vapour conductance g_{H_2O} (**c**)) and signals of selected VOCs (**d-f**) measured in leaf cuvette experiments simulating light-to-dark transitions. The sample plants were grown under different climate scenarios: elevated control (EC, solid line), chronic stress (CS, dotted line) and chronic stress recovery (CSr, dot-dashed line). The grey shaded area denotes a 10 min light period at the beginning of each experiment. After switching off the light, PIBs of several VOCs appeared such as acetaldehyde (**d**), isoprene (**e**), and the isomers Z-3-hexenal and E-2-hexenal (**f**). Under chronic stress PIBs were strongly suppressed. While PIBs of acetaldehyde were weaker in plants recovering from chronic heat and drought stress than in control plants, PIBs of GLVs like the hexenal isomers were enhanced. Signals are means of n=8 (EC) and n=4 (CS, CSr).
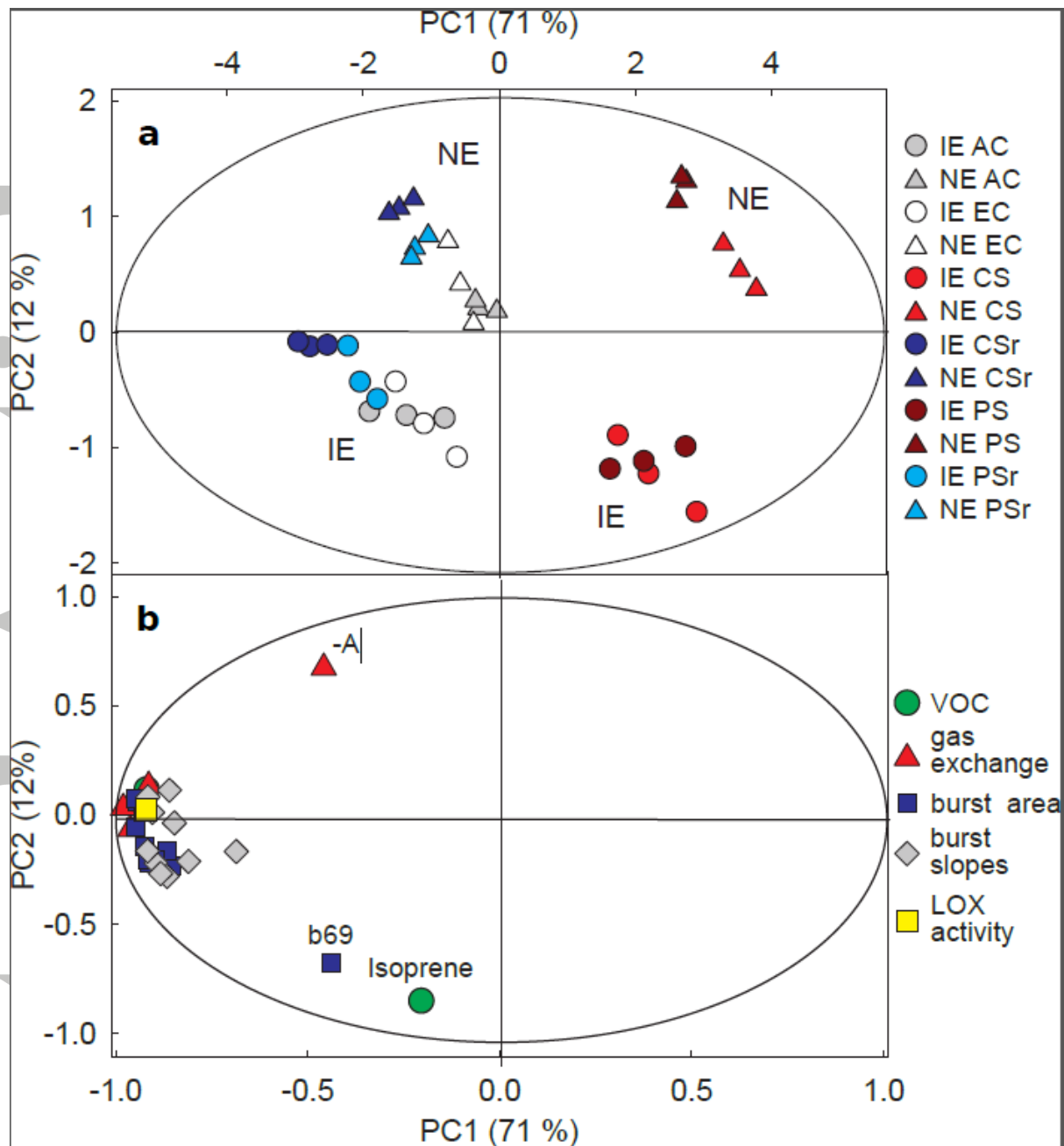
Figure 2: Score (**a**) and loading (**b**) plots of Principal Component Analysis (PCA) calculated using means of VOC bursts (integral of the peak curves), their slopes (through their rising edge), leaf-level VOC emission rates (of methanol and isoprene) during light conditions, gas-exchange parameters (net assimilation, dark respiration; transpiration under light condition; transpiration under dark condition) and *in-vitro* activities of LOX enzymes data. (**a**) IE (WT + PcISPS:GUS/GFP) circles; NE (RA1 + RA2), triangles. (**b**) Each parameter class is indicated by a different symbol. T2 ellipses denote a significance level of α = 0.05. Abbreviations used: IE: isoprene emitter, NE: isoprene non-emitter, AC: ambient control, EC: elevated control, CS: chronic stress, PS: periodic stress, CSr: chronic stress recovery, PSr: periodic stress recovery, -A: dark respiration, b69: burst area isoprene.
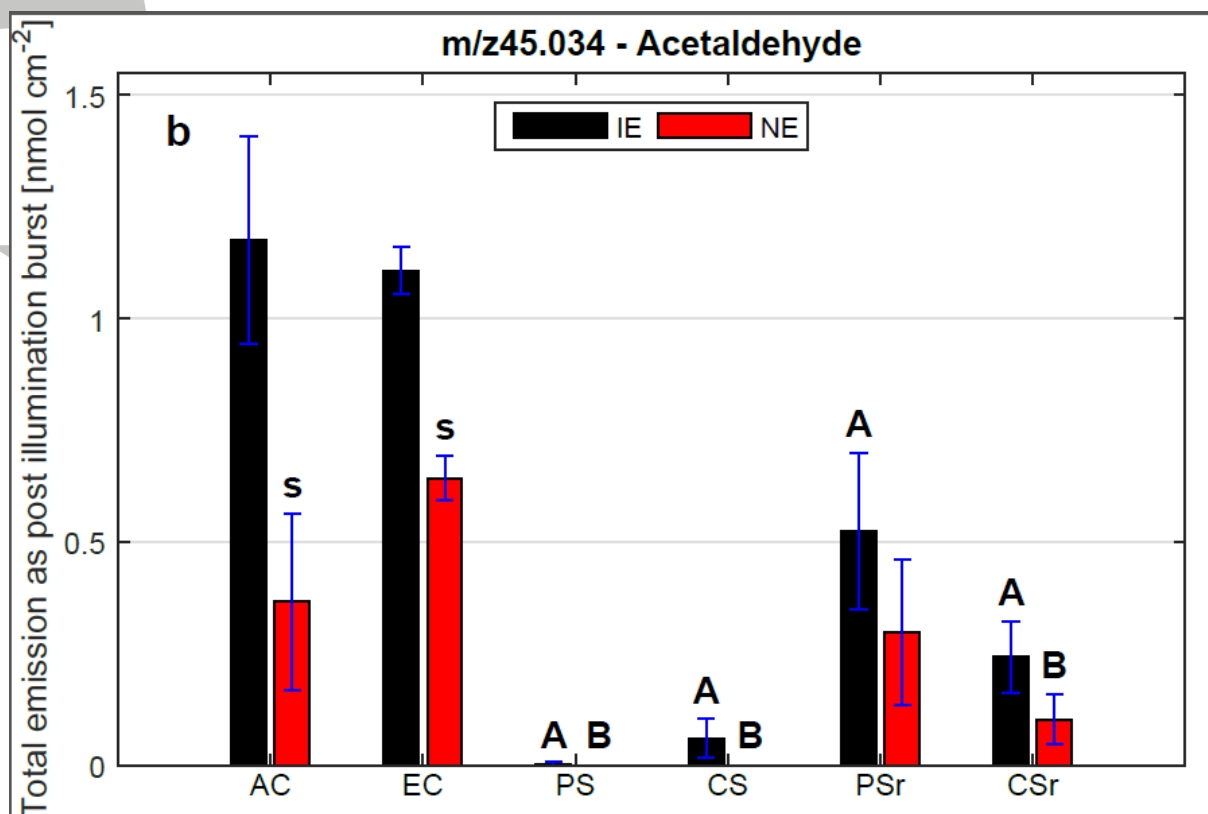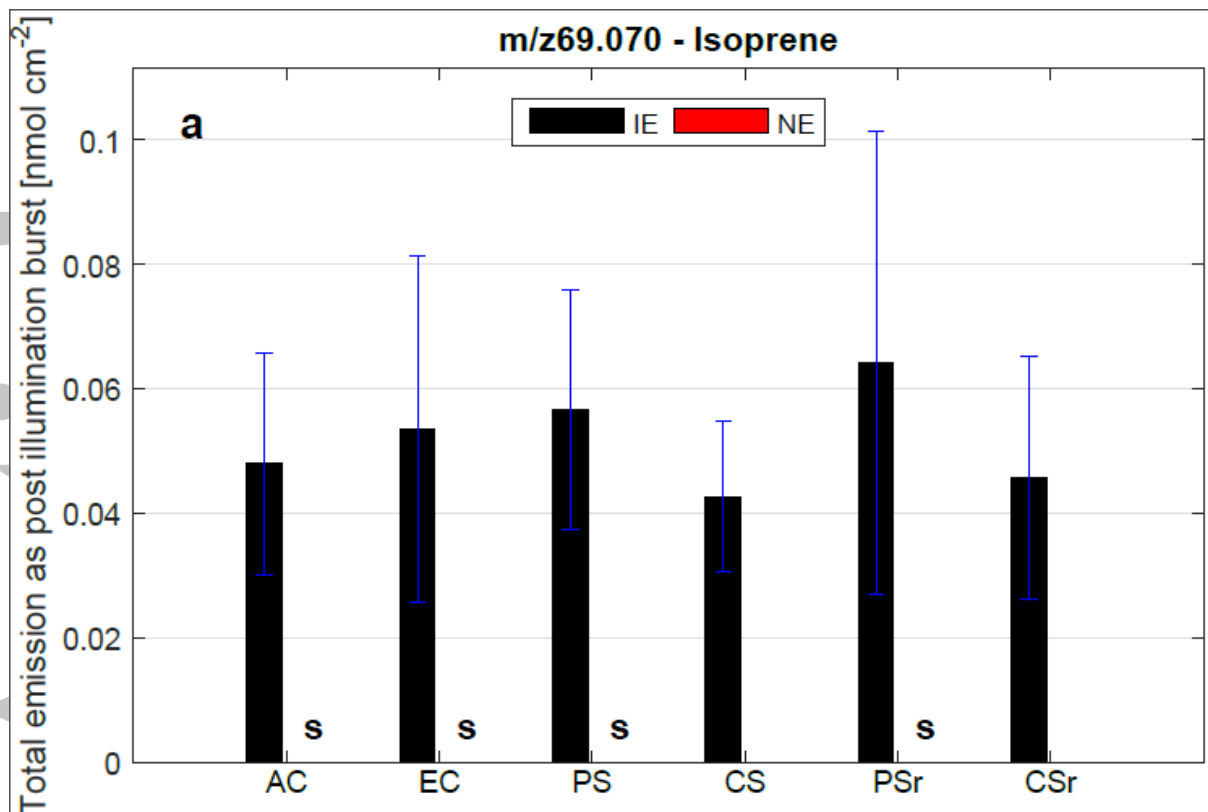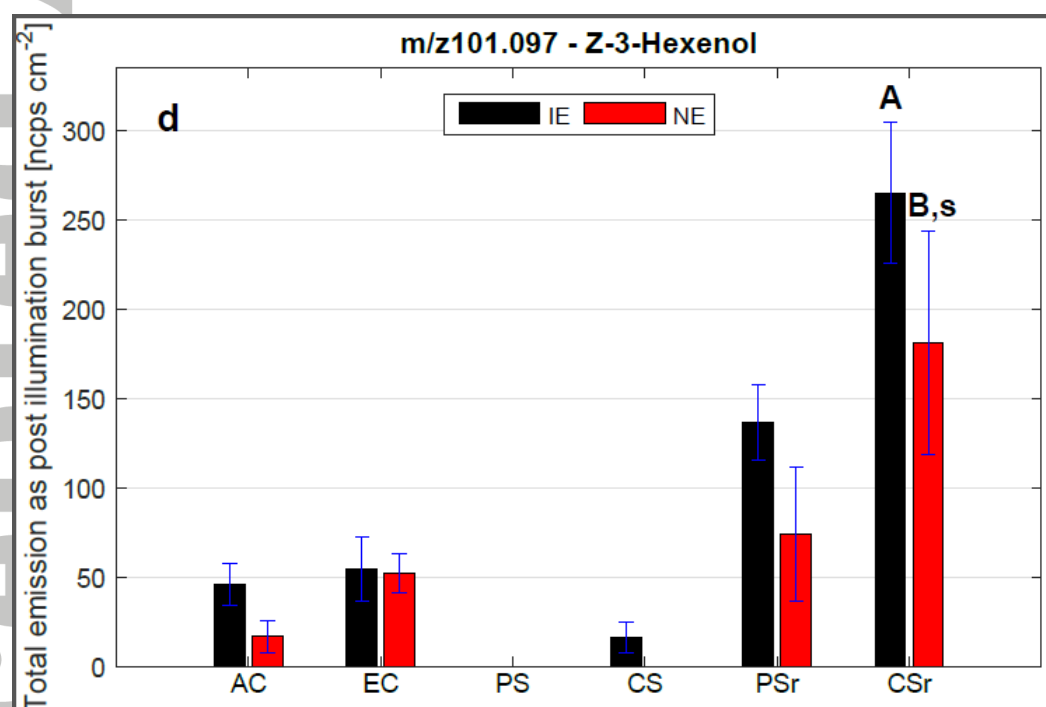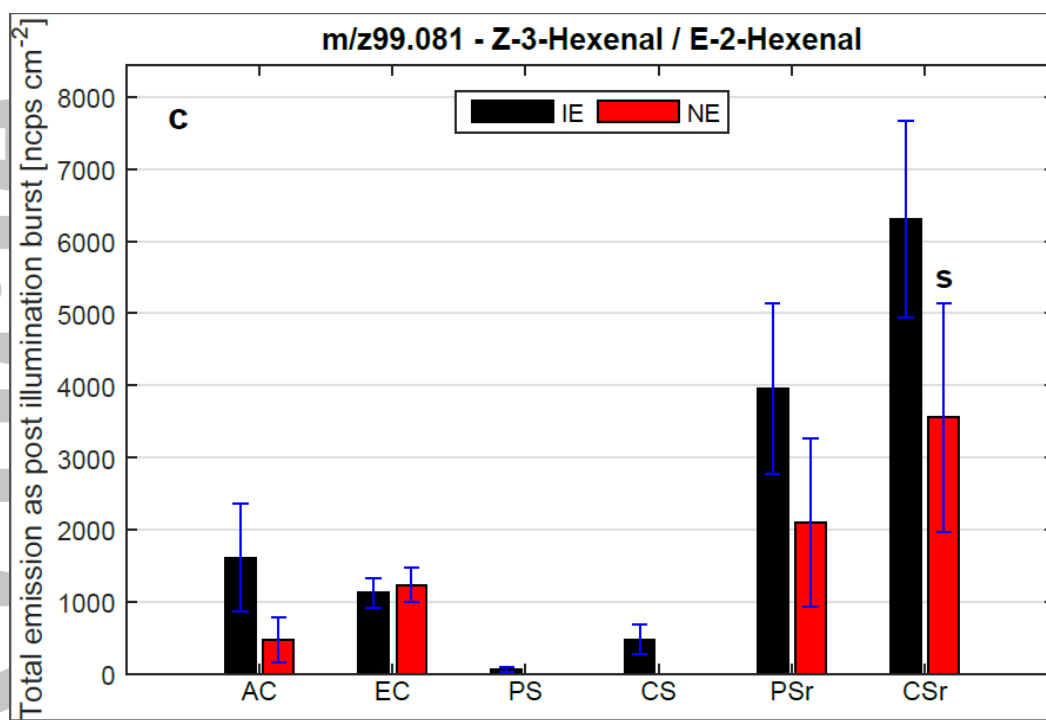
Figure 3: Mean total emissions (± s.e.) of isoprene (**a**) and selected oxygenated VOCs (**b**-**d**) in form of PIBs. In the PS and CS scenario all PIBs except those of isoprene were strongly suppressed. NE species generally showed less intense PIBs of oxygenated VOC than IE species. PIBs of the C_2 compounds like acetaldehyde were less intense in the stress recovery treatments (PSr and CSr) than in the corresponding control treatment (EC). Contrary, PIB of C_6 compounds like hexenal and hexenol were enhanced in plants recovering from HDS. Letters denote statistically significant (P<0.05) different values: (s) between IE and NE plants within the climate scenario, (A) in regard to the control treatment (EC) within IE plants and (B) in regard to the control treatment within NE plants (cf. Supplemental table S1).
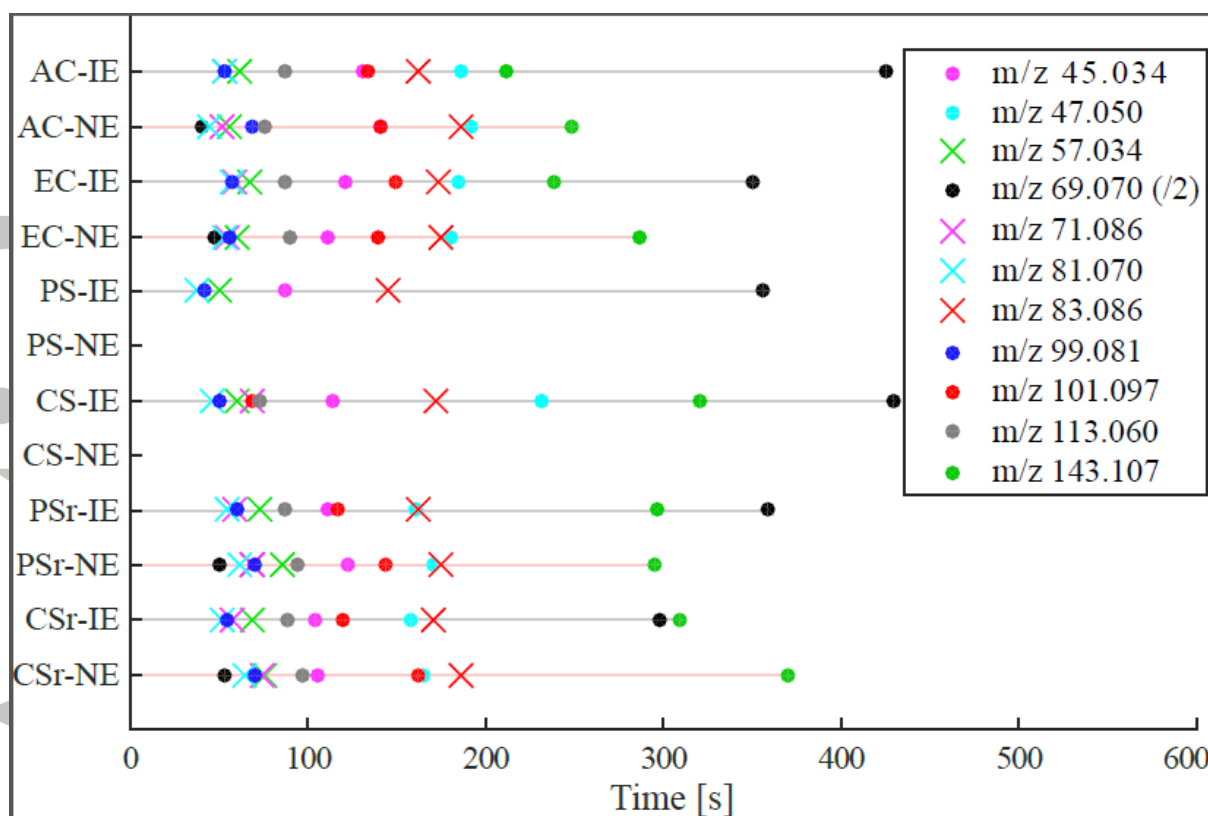
Figure 4: Mean time delays (expressed in seconds) after which the individual PIB maxima appeared after light-to-dark transitions (t = 0 s) in the different climate scenarios. Solid circles represent parent ions, while crosses represent known fragments. Values of m/z 69.070 were divided by two.
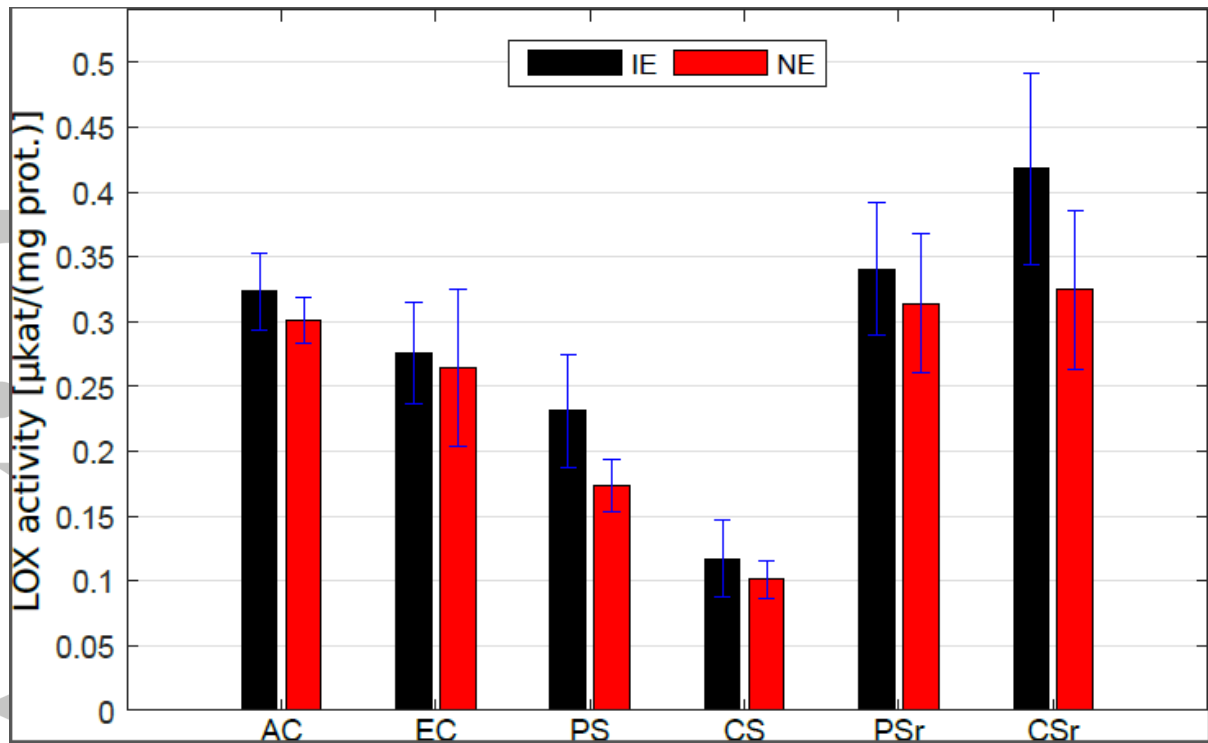
Figure 5: Mean activity of LOX enzymes (± s.e.) in isoprene emitting (IE) and isoprene non-emitting (NE) poplar plants in the different climate scenarios. In the chronic and periodic stress scenarios (CS and PS) the LOX activity was markedly reduced. Results of the statistical analysis are reported in Supplemental table S2.